sciendo

Polish Journal of Chemical Technology, 25, 4, 19—27, 10.2478/pjct-2023-0034

Numerical simulation and improvement of combustor structure in 3D printed sand recycling system

Xiao Gao, Mao Lei, Weiwei Xu*

College of New Energy, China University of Petroleum (East China), Qingdao 266580, China
Corresponding author: e-mail: xuweiwei@upc.edu.cn

In this paper, a new combustor with an output of 5 t/h is designed based on a computational particle fluid dynamics (CPFD) model. The flow field simulation is combined with the combustion simulation to analyze the internal two-phase flow, temperature field, and combustion products. The combustor structure was optimized. The simulation results show that the recovery efficiency of the waste sand and the energy utilization of the combustor can be improved under the original structure. The sand bed has a significant effect on flow field characteristics. The increase in particle temperature in the combustor increases the efficiency of waste sand recovery by increasing the height of the sand bed by 50 mm. The utilization rate of natural gas is increased and the economic efficiency is improved. The feasibility of the CPFD method can simulate the flow field characteristics inside the combustor very effectively.

Keywords: 3D printing; CPFD; thermal reclamation of used sand.

INTRODUCTION

3D printing is a new technology that uses data recorded in the computer and then accumulates the material layer by layer to produce physical objects, which has been used as an additional material manufacturing by academia. 3D printing involves a variety of equipment, materials, etc., and has been widely used in various industries such as biology, aerospace and so on[1]. Sand molds play a crucial role in 3D printing technology[2]. Sand casting is an economical and practical metal--forming process, which has been used since the Shang Dynasty in China[3]. The benefits of 3D printing for the casting industry were identified early[4, 5]. Foundry sand is commonly used in casting processes. In China's foundry industry, an average of 40 million tons of castings are produced annually. However, about 1.3 tons of solid waste will be produced by one ton of castings, of which sand and cores account for 40%–60%[6]. These used sand are found to be recyclable, minimizing production costs and environmental impact[7].

The reclamation of used sand is necessary, whether from the aspects of resource conservation or environmental protection. At present, the main reclamation processes of used foundry sand include dry, wet, and hot reclamation processes, thermal reclamation is the most widely accepted mode of sand reclamation[8]. Moreover, thermal reclamation is the most effective method for using sand with binders attached to the surface. This recycling method is based on the thermal degradation of the binder under high-temperature conditions to remove the binder on the surface of the used sand and achieve the effect of recycling the used sand[9, 10]. Meanwhile, the thermal regeneration process is a method of utilizing used molding and core sand that is more expensive than other recycling processes, but in most cases, it provides higher--quality recycled sand[11]. Temperature and the structure of the equipment are the two main factors affecting the thermal regeneration process[12]. Therefore, the structural optimization of the combustor is very important to save the energy consumption of sand recovery. Although it is difficult to achieve the above objectives, numerical calculation is an effective method.

The Computational Particle Fluid Dynamics (CPFD) model is used to simulate the combustor flow field, which is an Euler-Lagrangian model of two-phase gas-solid flow. In the CPFD method, the gas phase is considered a continuous phase and calculated in a single computational grid by the local average Navier-Stokes equation, while the solid phase is considered a discrete particle phase. The particle momentum model is based on the numerical description of the multiphase particle-in-cell (MP-PIC), which can handle the particle type and particle size distribution well[13–16]. Computational particles, also known as "parcel of particle", were introduced. Computational particles in the CPFD model were defined as combinations of a large number of real particles with similar properties, such as particle type, size, and density. The model traces a single "parcel of particle" rather than a single particle and calculates collisions between a large number of "parcel of particle" rather than between particles. Therefore, a small number of particles can be used to represent a gas-solid system with a large number of particles, which can significantly improve the simulation efficiency[17–19]. In recent years, the CPFD scheme has been widely used to analyze fluidized beds[20], bubbling beds[21, 22] and cold pilot calciner[23] due to the superiority of the CPFD model in particle simulation. Liu et al[24]. investigated the gas-solid flow characteristics of circulating fluidized beds, which has reference significance for further research on circulating fluidized beds. Shi et al.[25] pointed out that the outlet geometry of the riser can significantly affect flow hydrodynamics and solids back-mixing behaviors. Wang et al.[26] showed that the main benefit of the CPFD method was its capability to accurately predict the particle size distribution. In addition, extensive work compares the simulation data under different models (drag models, turbulent models, etc.) and model parameters (coefficients for particle--particle interactions and particle-wall interactions, etc.) in detail, indicating that it has a significant impact on the final simulation results[27–29].

CPFD method has been used in gas-solid flow studies many times and has also been proven to be applicable to various equipment. Although research on the combustors' performance has been carried out, these researches were mainly focused on the flow characteristics of combustors. The fluidization and combustion are rarely studied and have not been described in detail. In this

paper, the internal flow field of the combustor in the thermal regeneration system of waste sand is simulated by the CPFD method on the basis of considering the combustion characteristics. The characteristics of the internal flow field are revealed, the structure of the combustor is changed, and the internal flow fields under different structures are compared. The significance of these works is to optimize the combustor structure and combustion process. The purpose is to improve the recovery efficiency of used sand and the combustion efficiency of natural gas. Meanwhile, the feasibility of using CPFD for gas-solid flow predictions was verified. CPFD model was used for combustor simulation and was compared with the experiment.

THE CPFD MODEL

Governing equations

The volume average mass conservation equation for the continuous gas phase is

$$\frac{\partial \theta_g \rho_g}{\partial t} + \nabla \cdot \left(\theta_g \rho_g u_g\right) = 0 \tag{1}$$

The volume-average momentum conservation equation for the continuous gas phase is

$$\frac{\partial \left(\theta_g u_g \rho_g\right)}{\partial t} + \nabla \cdot \left(\theta_g \rho_g u_g u_g\right) = -\nabla P + \theta_g u_g \nabla^2 u_g + \theta_g \rho_g g - F \tag{2}$$

Where u_g represents the gas phase velocity, θ_g is the gas volume fraction, ϱ_g means the gas phase density, P is the gas phase pressure, g is the gravitational acceleration, and F is the unit volume gas-solid phase momentum exchange rate, which can be expressed as:

$$F = \iiint f V_p \rho_p \left[D\left(u_g - u_p\right) - \frac{1}{\rho_p} \nabla P \right] dV_p d\rho du_p \tag{3}$$

Where V_p is the particle volume, u_p is the particle velocity, ϱ_p is the particle density, and D is the drag function at the particle position.

Since the particle phase is described by the Lagrangian method, the particle is packaged using the concept of calculating particles, wherein the properties of the particles are the same. Therefore, the momentum equation of the particle can be expressed as:

$$\frac{du_p}{dt} = D_p\left(u_g - u_p\right) - \frac{1}{\rho_p} \nabla P + \frac{1}{\theta_g \rho_g} \nabla \tau_p \tag{4}$$

Where each represents gas phase drag, pressure gradient force, gravity, τ_p is normal stress gradient between particles.

The particle normal-stress model is described as[30]

$$\tau_p = \frac{P_s \theta_p^{\beta}}{\max\left[\left(\theta_{cp} - \theta_p\right) \cdot \varepsilon \left(1 - \theta_p\right)\right]} \tag{5}$$

Where P_S is the pressure and β is a constant (usually ranging from 2 to 5), θ_p is the particle volume fraction, ε is a small number of the order of 10^{-7}, and θ_{cp} is the particle volume fraction at close packing.

Gas-particle drag model

In the simulation of gas-solid two-phase flow, the drag model is used to describe the momentum exchange between gas-solid phase. Therefore, selecting the appropriate drag model is the key to accurate simulation of gas-solid phase flow. There are several commonly used drag models, namely the Wen&Yu model, the EMMS--Yang model, the Ergun model, and the Wen&Yu/Ergun model. It is reported that the Wen&Yu equation is confined to particle volume fraction from 0.01 to 0.61, while the Ergun equation is usually used from 0.47 to 0.7[31]. In the present work, the interphase gas-particle drag model is the Wen&Yu model. The corresponding drag model correlations are summarized as follows:

$$C_d = \begin{cases} \dfrac{24}{R_{ep}} \theta_g^{-2.65}, R_{ep} < 0.5 \\ \dfrac{24}{R_{ep}} \theta_g^{-2.65} \left(1 + 0.15 R_{ep}^{0.687}\right), 0.5 \le R_{ep} \le 1000 \\ 0.44 \theta_g^{-2.65}, R_{ep} > 1000 \end{cases} \tag{6}$$

Where R_{ep} is the Reynolds number, D_1 is Ergun interphase traction coefficient, d_p is Particle diameter.

NUMERICAL METHODS

The process flow diagram of the thermal reclamation system is shown in Figure 1. The whole process of the thermal regeneration system includes pretreatment of old sand, sand regeneration process, post-treatment of regenerated sand, and dust removal process, the most critical process is the sand regeneration process. The combustor is the most important equipment in the sand recovery process.

Structure of the combustor

The combustor used for simulation in this paper comes from a thermal reclamation of the used sand system. The three-dimensional diagram is shown in Figure 2. The lower part of the combustor is a pipe for transporting natural gas and air, and the upper part is a dust removal port. On the right side of the combustor is a sand inlet, and on the other side, a sand outlet is arranged at the lower part, and the whole combustor is very complicated.

Grid independence and comparison with experimental results

According to the characteristics of the multiphase flow of the combustor, Barracuda software based on CPFD method was used for simulation. The pipe model is meshed with a mesh number of 1.34 million, and the nozzle part and the smaller diameter part are locally encrypted to ensure the mesh quality as shown in Figure 3.

The main factors affecting the combustion process are temperature, time, reactants and combustion-supporting substances, etc., and temperature is also one of the two main factors affecting the heat recovery process. The simulation results are compared with the experimental results to demonstrate the feasibility of using CPFD to simulate the combustor as shown in Figure 4. The relationship between temperature and combustor position

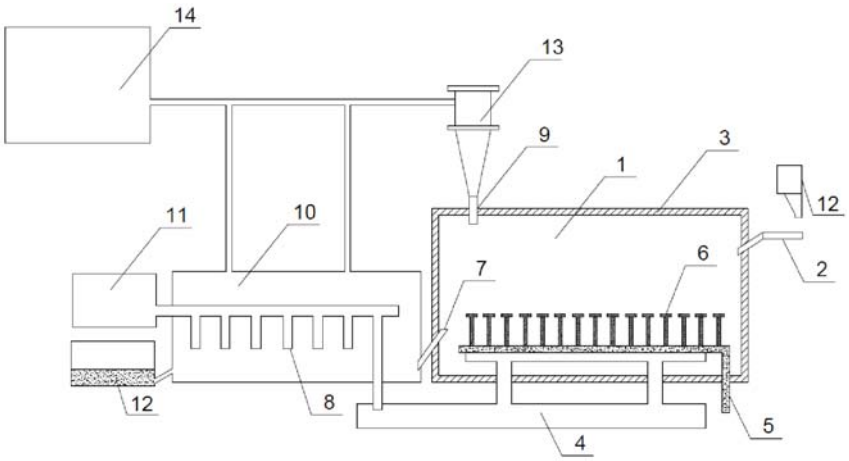

Figure 1. Process scheme of the thermal recovery system

1 – Combustor; 2 – Vibrating screen; 3 – Insulation; 4 – Air duct; 5 – Natural gas inlet; 6 – Combustion nozzle; 7 – Sand outlet; 8 – Air outlet; 9 – Dust removal port; 10 – Air cooling system; 11 – Cold air source; 12 – Screen; 13 – Water tower; 14 – Cyclone separator

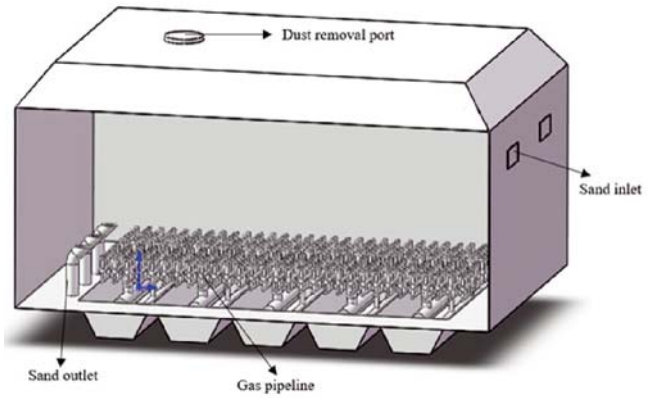

Figure 2. Three-dimensional structure of the combustor

is obtained by simulation results. The temperature on the right side is lower than the left side, which is due to the fact that the right side of the combustor is the sand inlet and has a lower temperature. By comparing with the experimental data, it can be seen that they have the same trend and the value is close, the temperature is maintained at about 800 K. Figure 4 indicates that the temperature is in good agreement with the experimental data. The experimental data are reference data obtained by comprehensive literature research. At x =1.335 m, the simulated temperature is 848 K and the experimental temperature is 835 K, which is 15 K higher than the experimental temperature and the relative experimental temperature error is 1.8%. At x = 3 m, the simulated

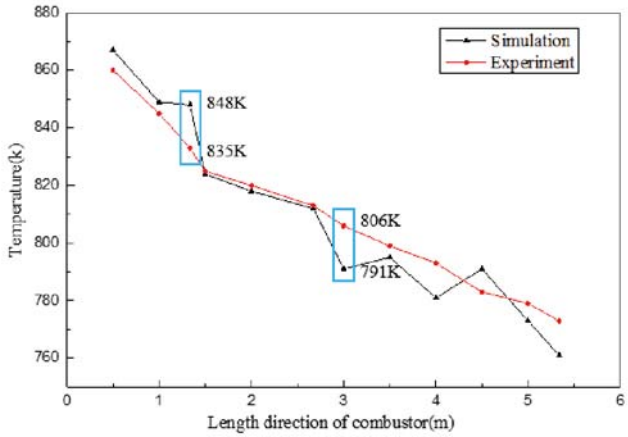

Figure 4. Temperature comparison for the numerical and experimental results in the combustor

temperature is 791 K and the experimental temperature is 806 K, the difference between experimental and simulated is 15 K, and the maximum difference between experimental and simulated is 15 K, the relative simulation error is 1.9%, which is within the theoretical error acceptance range, and it can be considered that there is good agreement between simulation and experiment to verify the simulation results.

Numerical procedures

The numerical simulation of the turbulent flow is solved by Large Eddy Simulation (LES), Euler-Lagrange

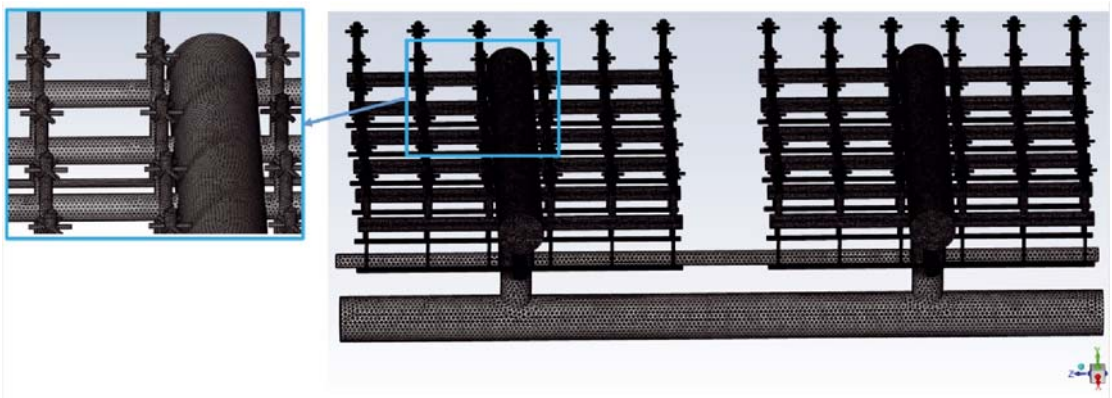

Figure 3. Meshing schematic of natural gas pipeline

Table 1. Simulation parameters

Parameters	Vale
Particle close pack volume fraction	0.68
Normal-to-wall momentum retention coefficient	0.30
Tangent-to-wall momentum retention coefficient	0.99
Initial pressure	101325 Pa
Gas	Natural gas and Air
Gas density	0.65 kg/m^3 and 1.205 kg/m^3
Natural gas inlet velocity	7.56 m/s
Natural gas temperature	430K
Air inlet velocity	21.25 m/s
Thermal air	480K
Inlet used sand flow rate	0.97kg/s
used sand temperature	425K
Chemistry coefficient	K=2.119e + 11e$^{-24380.6/T}$
Chemical equation	$CH_4 + 2O_2 \rightarrow CO_2 + 2H_2O$
Chemical reaction rate	R=K$(CH_4)^{0.2}(O_2)^{1.3}$
Sand inlet velocity	0.97 kg/s
Time step	0.003

method for gas-solid two-phase flow, and the calculation of the coupled pressure and velocity fields. The SIMPLE algorithm was chosen. The turbulent flow and combustion of the boiler are simulated and analyzed. The simulation parameters are shown in Table 1. The particles used the particle size distribution (PSD) shown in Table 2 which is used in the experiment. The particles are round to simplify the calculation. Most of the used sand particles are distributed between 109 and 270 μm in diameter. The bulk density of used sand is 1500 kg/m^3 and its density is 2200 kg/m^3. The used sand is laid in the lower part of the combustor in advance, and the height is about 50 ~100 mm below the sand outlet, the gas entering the combustor is preheated in advance. Air and natural gas react completely to form carbon dioxide and water (gaseous water at high temperatures) during combustion, the chemical reaction rate coefficient equation is as follows:

$$D_1 = 0.75 C_d \frac{\rho_g |u_g - u_p|}{\rho_p d_P} \tag{7}$$

Among them, C_0, C_1, C_2, C_3, and C_4, are all coefficients, and E is activation energy.

Based on previous research and the setting of natural gas combustion in Fluent software, C_0 = 2.119e + 11, E = 24380.6. It is automatically saved every 20 steps during the simulation.

Table 2. Particle size distribution of the used sand

Diameter of the used sand (ĕm)	Accumulative fraction of weight for particle with diameter (%)
270	100
109	10
85	5
62	0
The density of the used sand, 2200 kg/m^3	

RESULTS AND DISCUSSION

Analysis of flow field characteristics in the combustor

The initial conditions and boundary conditions are set to obtain the flow field characteristics of the fluid and the particles based on the CPFD model. The following is the simulation result analysis.

The above three figures show the gas distribution in the combustor. The natural gas content is high at the inlet, the middle part is free of natural gas, and the natural gas that has not yet reacted is present in the upper space of the combustor as can be seen in Figure 5. In addition, the middle part of the combustor contains the most carbon dioxide, and the upper and inlet parts are basically free of carbon dioxide as shown in Figure 6, which reveals that the combustion reaction is mainly concentrated in the middle part of the combustor. Figure 7 indicates that the oxygen content is sufficient throughout the combustion reaction and that a large amount of oxygen remains after the reaction. According

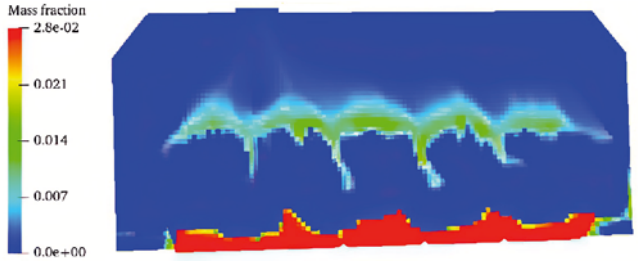

Figure 5. Contour of natural gas distribution in the combustor

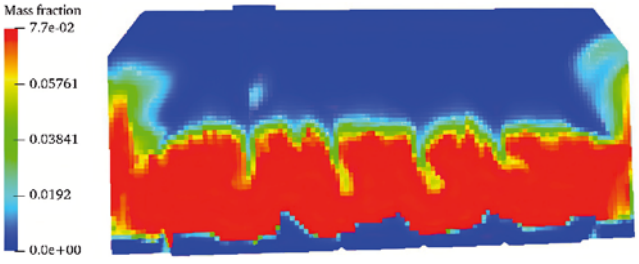

Figure 6. Contour of carbon dioxide distribution in the combustor

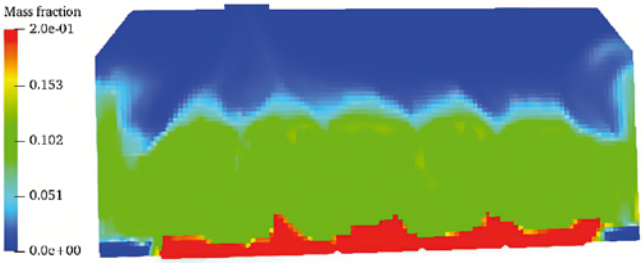

Figure 7. Contour of oxygen distribution in the combustor

to the chemical reaction equation, the remaining natural gas and oxygen can continue to react.

The distribution of particle volume fraction in the combustor is shown in Figure 8. Since the gas injected from the air inlet has an upward velocity and is greater than the minimum fluidization velocity, the originally static used sand particles are fluidized. The binder on the surface of the used sand is removed by the combustion reaction of natural gas with oxygen. Under natural conditions, the stacking volume fraction of the used sand particles is 0.68. The volume fraction of the particles maintains the value in the portion of the combustor where there is no nozzle. The larger volume fraction is located in the middle of the combustor and the periphery is smaller, in some places even zero in the part with the nozzle. The used sand coming from the sand inlet is subjected to an upward force due to the gas moving from the bottom to the top. A vortex is generated below the sand inlet due to the combined effect of other forces leading to a change in the trajectory of the used sand.

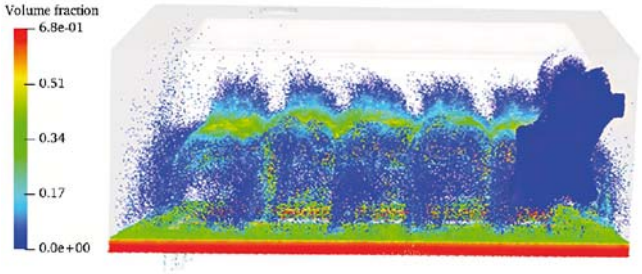

Figure 8. Particles volume fraction distribution in the combustor

The velocity distribution of the used sand particles in the combustor is shown in Figure 9. The velocity of the upper particles of the combustor tends to zero, indicating that most of the particles have risen to the highest point. The larger particles begin to move downward, while the smaller particles continue to move upward and eventually out of the combustor through the upper dust removal port. The particles in the lower layer of the combustor still have an upward velocity and continue to move upwards.

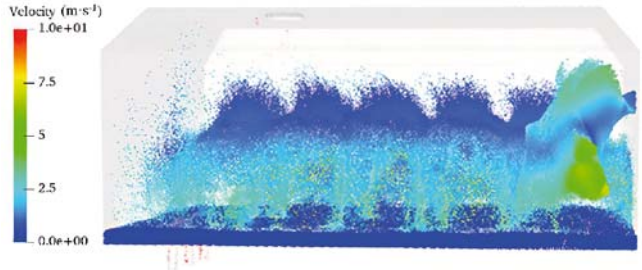

Figure 9. Particles velocity distribution in the combustor

Natural gas reacts with oxygen to form carbon dioxide and gaseous water as the reaction proceeds. Natural gas flows out of the combustor from the dust removal port at about 0.25 seconds from Figure 10. This part of the natural gas does not react before the time, which causes a waste of energy and a decrease in the economic efficiency of the whole recovery system. It should be noted that proper temperatures are required to remove the binder from the surface of the old grit by combustion reactions besides sufficient air and natural gas.

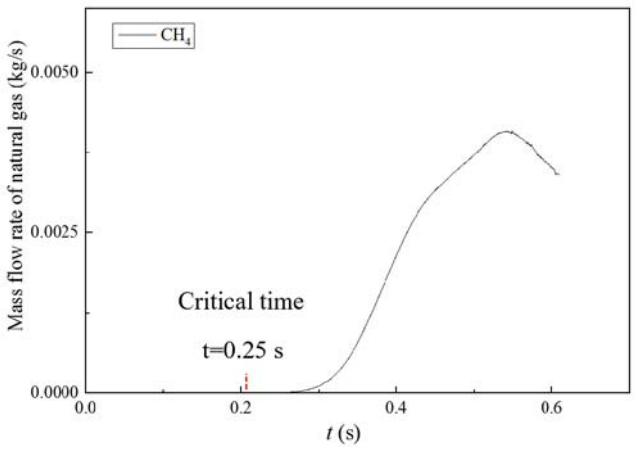

Figure 10. Mass flow rate of natural gas discharged from the dust removal port

The particle temperature distribution and particle position in the combustor are shown in Figure 11. The temperature of most of the particles is maintained between 900 K and 1000 K, except for the bottom and the used sand particles that have just entered the combustor from the sand inlet. The temperature required to remove the binder on the surface of the particles is above 873 K. The results show that most of the particle temperatures have reached this standard. It is necessary to bring the generated high-temperature zone close to the sand layer to better utilize the heat generated by natural gas combustion, which can improve heat utilization and achieve energy savings.

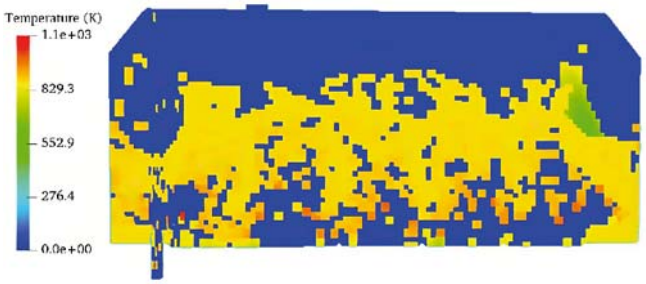

Figure 11. Temperature distribution of used sand particles in the combustor

The temperature distribution inside the combustor is shown in Figure 12. The bottom space and sand inlet of the combustor appear as low-temperature areas due to the entry of gas and used sand particles. The intense local combustion causes the internal space to reach a maximum temperature of 1800 K. In addition, the overall temperature of the combustor is maintained at about 1000 K, which coincides with the distribution region of the used sand particles. The results show

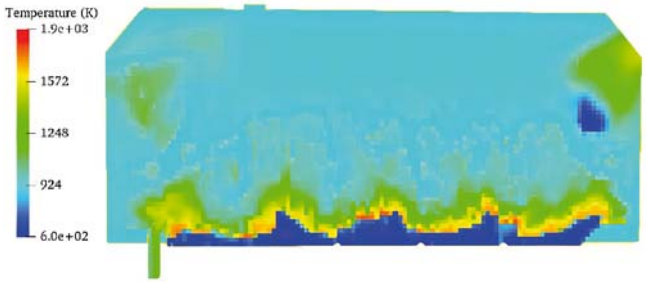

Figure 12. Temperature distribution of the flow field in the combustor

that the binder on the surface of the particles can be effectively combusted.

Analysis of combustor improvement

The effect of the combustor geometry on the internal flow field is discussed by changing the structure of the combustor and comparing it with the original structure. The change in the slope of the sand inlet directly affects the feed velocity. The slope of the combustor inlet is changed to 45 degrees and 60 degrees, and the inlet is moved up and down by 100 mm and 200 mm, while the outlet is moved up and down by 50 m, respectively. The structure of the combustor was improved to achieve better removal of the binder from the surface of the old sand and also to save natural gas energy.

For the convenience of description, (1) to (9) represent the original structure, the angle of the sand inlet is 45 degrees, the angle of the sand inlet is 60 degrees, the sand outlet is increased by 50 mm, the sand outlet is decreased by 50 mm, the sand inlet is increased by 100 mm and 200 mm, the sand inlet decreased by 100 mm and 200 mm, respectively.

The change in the combustor structure has a corresponding effect on the particle volume fraction as can be seen from Figure 13. The distribution of used sand particles in its internal space is similar, but the degree of fluidization of particles is higher than in other structures with the height of the sand outlet increasing by 50 mm. The height of the initial sand layer increases as the height of the sand outlet increases, which can improve particle fluidization.

The distribution of natural gas inside the combustor is shown in Figure 14. The structural improvement of the combustor has little effect on the distribution of the various gases. The distribution of gases is similar under all structures, including carbon dioxide and oxygen. Na-

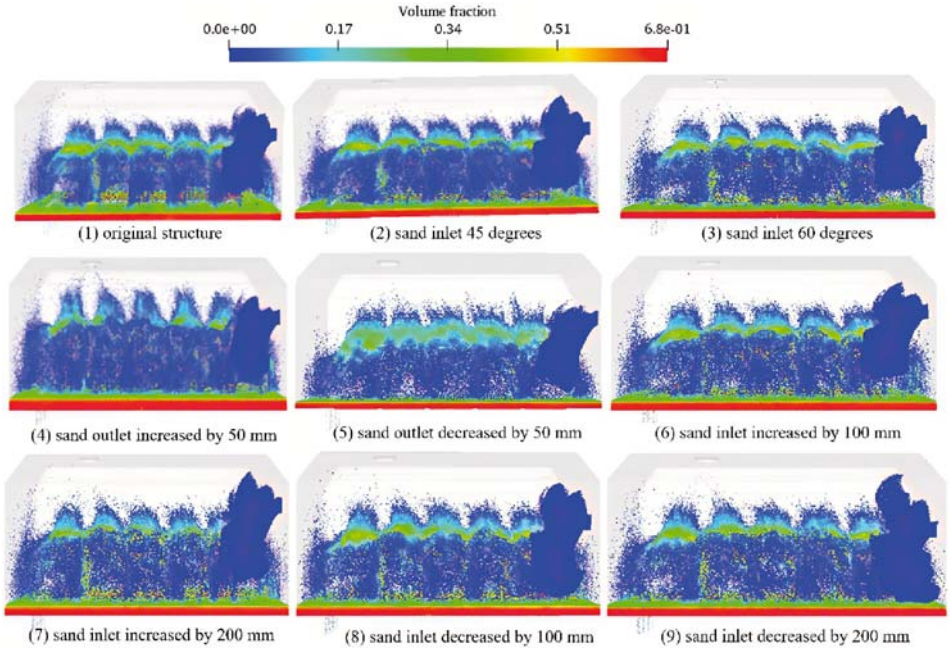

Figure 13. Particles volume fraction distribution in the combustor with different structural parameters

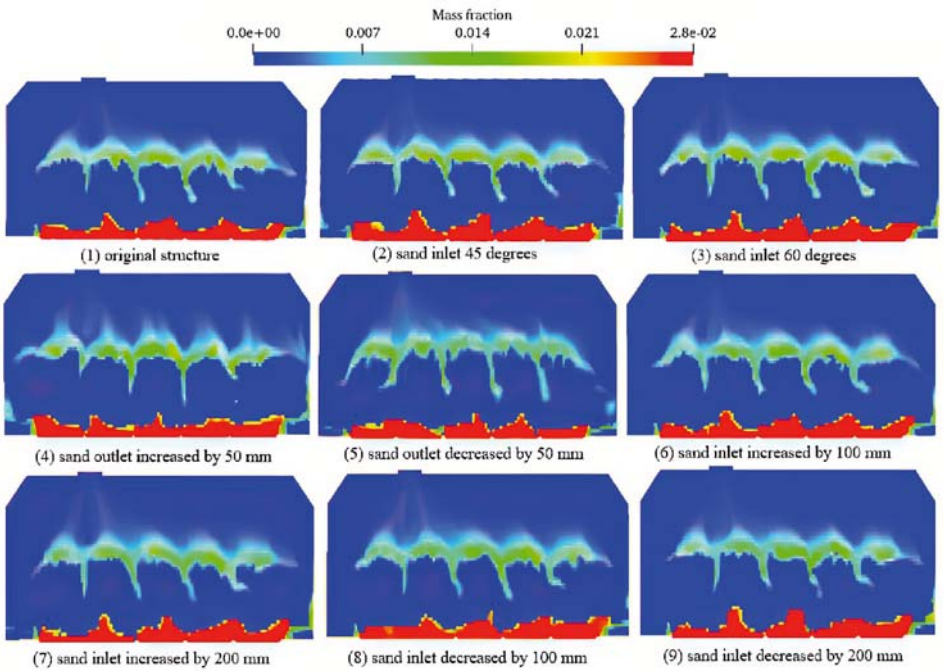

Figure 14. Contours of natural gas distribution in combustor with different structural parameters

tural gas is distributed both at the bottom and at the top and there is natural gas flowing out of the combustor through the dust removal port, resulting in a waste of natural gas. Carbon dioxide is mainly distributed in the middle, and the amount of oxygen is always sufficient during the reaction.

The variation of the percentage of natural gas leaving the combustor has the same trend under all structures as shown in Figure 15. However, the proportion of natural gas at the same time is smaller than that of the other structures after 0.35 seconds as the sand outlet raised by 50 mm. The proportion of natural gas leaving the combustor is smaller, which can achieve the effect of saving natural gas.

Temperature is one of the two main factors affecting the thermal regeneration process during the combustor working, which is related to the quality of the regenerated sand. The change of combustor structure also affects the internal temperature distribution.

The temperature distribution of the fluid and particles inside the combustor is shown in Figure 16 and Figure 17. The overall temperature inside the combustor is kept around 1000 K, and the temperature of the particles is around 900 K. The low-temperature region exists at the bottom and inlet area of the sand. The high-temperature region of the fluid and the pellet region basically overlap under various structures, which is favorable for improving heat utilization efficiency. Among them, the 3rd, 4th, 6th, and 8th diagrams show that the temperature of the particles is higher than the temperature of the other structures so it is advantageous to completely remove the binder from the surface of the used sand particles.

In summary, the height of the sand outlet is increased by 50 mm, which can improve the temperature of the particles make the quality of the recycled sand better, and also reduce the waste of natural gas, and improve the efficiency of heat utilization. The combustion

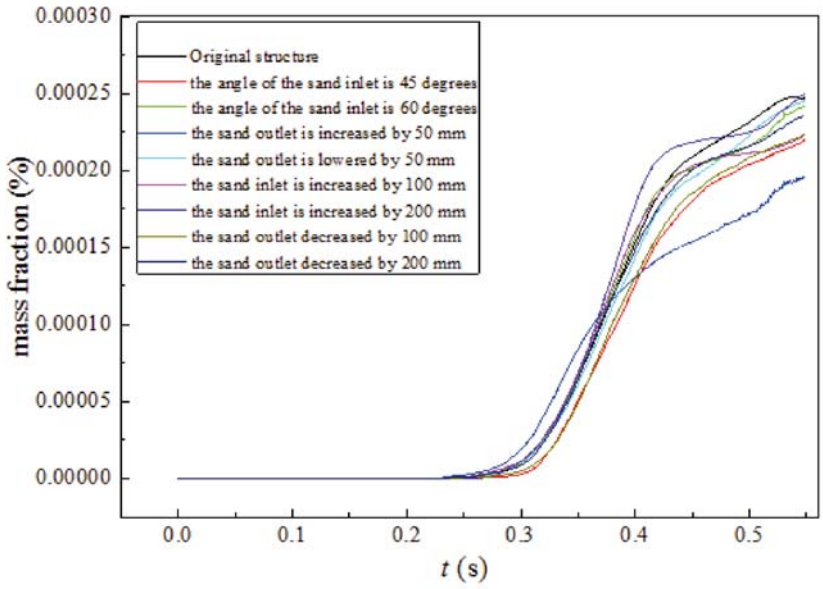

Figure 15. Comparison of the mass fraction of natural gas flowing from the dust removal port for combustor of different structures

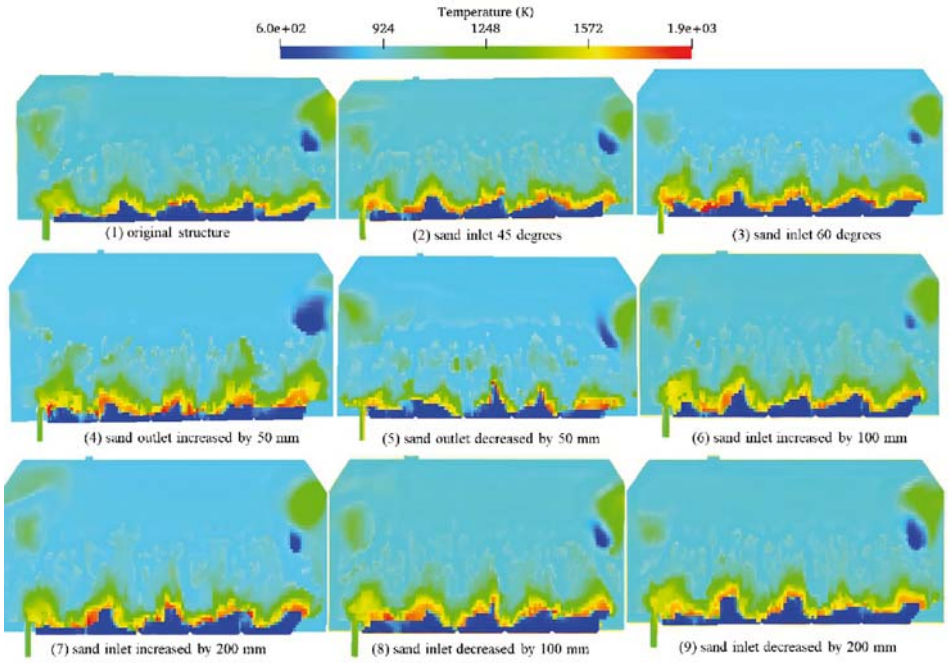

Figure 16. Contours of flow field temperature distribution in the combustor with different structural parameters

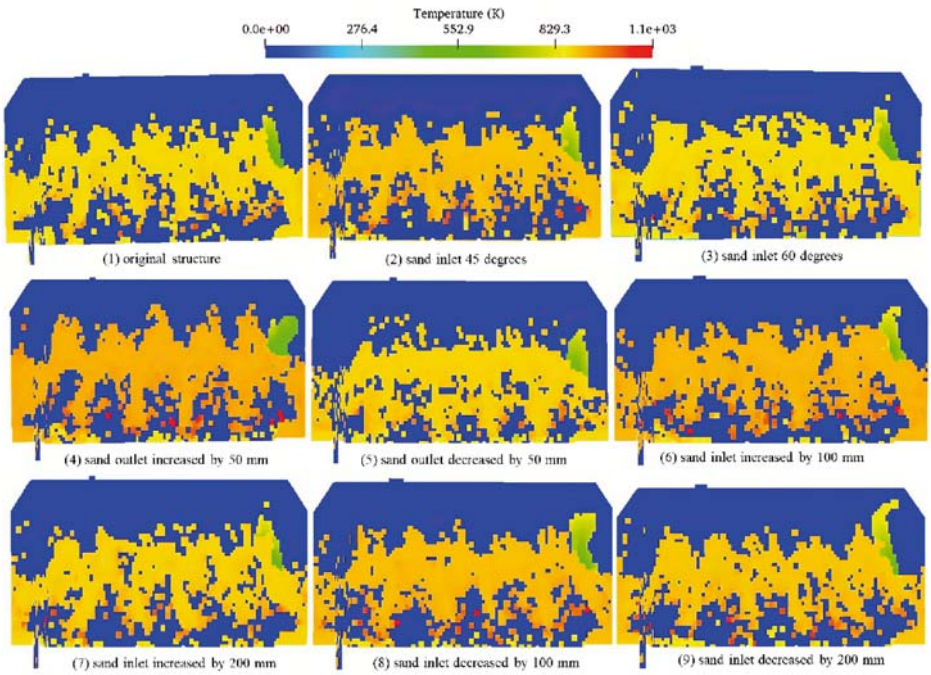

Figure 17. Contours of particles temperature distribution in the combustor with different structural parameters

optimization effect of changing the height of the sand outlet is the best.

CONCLUSIONS

The combustor is one of the most important pieces of equipment in the thermal reclamation system. Temperature and equipment structure are the two main factors affecting the thermal reclamation process, and the equipment structure affects the temperature distribution. It is necessary to have an exhaustive understanding of the flow characteristics of the combustor. The current work uses the CPFD method for numerical simulation. Flow field characteristics and combustor structure optimization were analyzed to obtain the following conclusions:

(1) The CPFD method can well simulate the flow field characteristics inside the combustor, and the feasibility of gas-solid two-phase flow prediction has been verified.

(2) The recovery efficiency and energy utilization of waste sand can be improved by the analysis of the flow field characteristics inside the combustor. The simulation results indicate that parameters such as the height of the sand outlet, the height of the sand inlet, and the sand feeding speed can all affect the recovery process, especially the height of the sand outlet, which has a significant impact on the internal flow field characteristics.

(3) The optimized structure method of the combustor with known output of 5 t/h is to increase the height of the sand outlet by 50 mm and the height of the sand bed from the original 250 mm to 300 mm. The optimized combustor improves the temperature of the particles and the utilization rate of natural gas, which not only improves the recovery efficiency of the waste sand, but also improves the economic efficiency of the system.

(4) The combustor model used in this article is very complex, and the research method of combining combustion process with gas-solid two-phase flow has reference significance for combustor-related research.

Acknowledgments

Thanks to CNOOC Energy Development Equipment Technology Co., Ltd. for funding the article.

LITERATURE CITED

1. Ngo, T.D., Kashani, A., Imbalzano, G., Nguyen, K.T. Q. & Hui, D. (2018). Additive manufacturing (3D .printing): A review of materials, methods, applications and challenges. *Comp. Part B: Engin*., 143, 172–196. DOI: 10.1016/j.compositesb.2018.02.012.

2. Upadhyay, M., Sivarupan, T. & El Mansori, M. (2017) 3D printing for rapid sand casting—A review. *J. Manufac. Proc.* 29, 211–220. DOI: 10.1016/j.jmapro.2017.07.017.

3. Walker, J., Harris, E., Lynagh, C., Beck, A., Lonardo, R., Vuksanovich, B., Thiel, J., Rogers, K., Conner, B. & MacDonald, E. (2018) 3D Printed Smart Molds for Sand Casting. *Internat. J. Metalc*., 12(4), 785–796. DOI: 10.1007/s40962-018-0211-x.

4. C. Hull., M. Feygin., Y. Baron., R. Sanders., E. Sachs., A.Lightman. & T. Wohlers. (1995). Rapid prototyping:current technology and. *Rapid Prototyp. J*., 1, 11–19.

5. Wang, J., Sama, S.R. & Manogharan, G. (2018). Re--Thinking Design Methodology for Castings: 3D Sand-Printing and Topology Optimization. *Internat. J. Metalc*., 13(1), 2–17. DOI: 10.1007/s40962-018-0229-0.

6. Ying-Min, L., Tian-Shu, W. & Wei-Hua, L. (2018). Research on regeneration methods of animal glue waste sand for foundry. *R Soc. Open Sci*., 5(5), 172270. DOI: 10.1098/rsos.172270.

7. Andrade, R.M., Cava, S., Silva, S.N., Soledade, L.E.B., Rossi, C.C., Roberto Leite, E., Paskocimas, C.A., Varela, J.A. & Longo, E. (2005). Foundry sand recycling in the troughs of blast furnaces: a technical note. *J. Mat. Proces. Technol*., 159(1), 125–134. DOI: 10.1016/j.jmatprotec.2003.10.021.

8. Khan, M.M., Singh, M., Mahajani, S.M., Jadhav, G.N. & Mandre, S. (2018). Reclamation of used green sand in small scale foundries. *J. Mat. Proces. Technol*., 255, 559–569. DOI: 10.1016/j.jmatprotec.2018.01.005.

9. Lucarz, M. (2015). Setting temperature for thermal reclamation of used moulding sands on the basis of thermal analysis. METALURGIJA 54(2), 319–322.

10. Lucarz, M. (2015). Thermal reclamation of the used moulding sands. *METALURGIJA* 54(1), 109–112.

11. Łucarz, M., Grabowska, B. & Grabowski, G. (2014). Determination of Parameters of the Moulding Sand Reclamation Process, on the Thermal Analysis Bases. *Arch. Metal. Mat*., 59(3), 1023–1027. DOI: 10.2478/amm-2014-0171.

12. Łucarz, M. (2013). The Influence of The Configuration of Operating Parameters of a Machine for Thermal Reclamation on the Efficiency of Reclamation Process. *Arch. Metal. Mater*., 58(3), 923–926. DOI: 10.2478/amm-2013-0102.

13. Lanza, A., Islam, M.A. & de Lasa, H. (2016). CPFD modeling and experimental validation of gas–solid flow in a down flow reactor. *Comp. & Chem. Engin*., 90, 79–93. DOI: 10.1016/j.compchemeng.2016.04.007.

14. Chen, C., Werther, J., Heinrich, S., Qi, H.-Y. & Hartge, E.-U. (2013).CPFD simulation of circulating fluidized bed risers. *Powder Technol*., 235, 238–247. DOI: 10.1016/j.powtec.2012.10.014.

15. Snider, D.M., O'Rourke, P.J. & Andrews, M.J. Sediment flow in inclined vessels calculated using a multiphase particle-in-cell model for dense particle flows. *Internat. J. Multiphase Flow*., 24,(8), 1359–1382.

16. Snider, D.M. (2001). An Incompressible Three-Dimensional Multiphase Particle-in-Cell Model for Dense Particle Flows. *J. Comput. Physics*., 170(2), 523–549. DOI: 10.1006/jcph.2001.6747.

17. Abbasi, A., Ege, P.E. & de Lasa, H.I. (2011). CPFD simulation of a fast fluidized bed steam coal gasifier feeding section. *Chem. Engin. J*., 174(1), 341–350. DOI: 10.1016/j.cej.2011.07.085.

18. Lan, X., Shi, X., Zhang, Y., Wang, Y., Xu, C. & Gao, J. (2013). Solids Back-mixing Behavior and Effect of the Mesoscale Structure in CFB Risers. *Ind. & Engin. Chem. Res*., 52(34), 11888–11896. DOI: 10.1021/ie3034448.

19. Snider, D.M. (2007). Three fundamental granular flow experiments and CPFD predictions. *Powder Technol*., 176(1), 36–46. DOI: 10.1016/j.powtec.2007.01.032.

20. Zhao, P., O'Rourke, P.J. & Snider, D. (2009). Three-dimensional simulation of liquid injection, film formation and transport, in fluidized beds. *Particuology* 7(5), 337–346. DOI: 10.1016/j.partic.2009.07.002.

21. Snider, D. & Banerjee, S. (2010). Heterogeneous gas chemistry in the CPFD Eulerian–Lagrangian numerical scheme (ozone decomposition). *Powder Technol*., 199(1), 100–106. DOI: 10.1016/j.powtec.2009.04.023.

22. Karimipour, S. & Pugsley, T. (2012). Application of the particle in cell approach for the simulation of bubbling fluidized beds of Geldart A particles. *Powder Technol*., 220, 63–69. DOI: 10.1016/j.powtec.2011.09.026.

23. Nakhaei, M., Hessel, C.E., Wu, H., Grévain, D., Zakrzewski, S., Jensen, L.S., Glarborg, P. & Dam-Johansen, K. (2018). Experimental and CPFD study of gas–solid flow in a cold pilot calciner. *Powder Technol*., 340, 99–115. DOI: 10.1016/j.powtec.2018.09.008.

24. Liu, H., Li, J. & Wang, Q. (2017). Simulation of gas–solid flow characteristics in a circulating fluidized bed based on a computational particle fluid dynamics model. *Powder Technol*., 321, 132–142. DOI: 10.1016/j.powtec.2017.07.040.

25. Shi, X., Wu, Y., Lan, X., Liu, F. & Gao, J. (2015). Effects of the riser exit geometries on the hydrodynamics and solids back-mixing in CFB risers: 3D simulation using CPFD approach. *Powder Technol*., 284, 130–142. DOI: 10.1016/j.powtec.2015.06.049.

26. Wang, Q., Niemi, T., Peltola, J., Kallio, S., Yang, H., Lu, J. & Wei, L. (2015). Particle size distribution in CPFD modeling of gas–solid flows in a CFB riser. *Particuology* 21, 107–117. DOI: 10.1016/j.partic.2014.06.009.

27. Benyahia, S., Syamlal, M. & O'Brien, T.J. (2005). Evaluation of boundary conditions used to model dilute, turbulent gas/solids flows in a pipe. *Powder Technol*., 156(2-3), 62–72. DOI: 10.1016/j.powtec.2005.04.002.

28. Almuttahar, A. & Taghipour, F. (2008). Computational fluid dynamics of high density circulating fluidized bed riser: Study of modeling parameters. *Powder Technol*., 185(1), 11–23. DOI: 10.1016/j.powtec.2007.09.010.

29. Li, T., Dietiker, J.F. & Shadle, L. (2014). Comparison of full-loop and riser-only simulations for a pilot-scale circulating fluidized bed riser. *Chem. Engin. Sci*., 120, 10–21. DOI: 10.1016/j.ces.2014.08.041.

30. Harris, S.E. & Crighton, D.G. (1994). Solitons, solitary waves, and voidage disturbances in gas-fluidized beds *J. Fluid Mech*., 266, 243–276.

31. Shi, X., Sun, R., Lan, X., Liu, F., Zhang, Y. & Gao, J. (2015). CPFD simulation of solids residence time and back-mixing in CFB risers. *Powder Technol*., 271, 16–25. DOI: 10.1016/j.powtec.2014.11.011.